Adsorption of Congo Red Dye from Aqueous Solution using ZnO and Al₂O₃/ZnO Composite: Isotherm, Kinetic and Thermodynamic Data

[1*]BELLO, MO; [2]OYEWUMI-MUSA, RT; [1]ABDUS-SALAM, N; [1]GBENRO, MT; [1]EGBENEYE, OG

[1]Department of Chemistry University of Ilorin, Ilorin, Kwara State, Nigeria
[2]Department of Chemical and Geological Sciences, Al-Hikimah University, Ilorin, Ilorin, Kwara State, Nigeria
Corresponding Author Email: bello.mo@unilorin.edu.ng

ABSTRACT: Herein, an adsorption study of congo red (CR) dye onto ZnO and Al₂O₃/ZnO is reported. ZnO was prepared using conventional chemicals by co-precipitation method and Al₂O₃ used in the composite was prepared through recycling of aluminium waste. Information about the materials was obtained through spectroscopic techniques. A batch adsorption method was used to obtain the adsorption data from which isotherm, kinetic and thermodynamic parameters were obtained. The result of the adsorbents characterisation revealed the expected properties of the prepared materials. The adsorption capacities at 250 mg/L of CR dye were 24.33 mg/g and 24.57 mg/g for ZnO and Al₂O₃/ZnO respectively. The isotherm study of the adsorption process revealed that Langmuir model fitted best the adsorption data with monolayer adsorption capacities (q_m) of 27.67 mg/g and 33.39 mg/g for ZnO and Al₂O₃/ZnO respectively. The adsorption was rapid within the first 15 min and the equilibrium was reached at 45 min. The kinetic study followed a pseudo-second-order model with the rate constant of 0.049 and 0.093 g.mg^{-1}.min^{-1} for ZnO and Al₂O₃/ZnO respectively. Experimentally, the process was endothermic and was supported by the positive values of enthalpy (ΔH) with positive values of entropy (ΔS). The change in free energy (ΔG) is negative at all temperatures studied, indicating spontaneity but more spontaneous for Al₂O₃/ZnO than ZnO. The adsorption of CR dye from an aqueous solution onto ZnO as an adsorbent can be slightly improved upon by the introduction of Al₂O₃ to form Al₂O₃/ZnO composite.

Impact factor: http://sjifactor.com/passport.php?id=21082

Google Analytics: https://www.ajol.info/stats/bdf07303d34706088fffffbc8a92c9c1491b12470

Water is an indispensable resource that is essential for life development (Lellis *et al*., 2019). Its contamination or pollution poses a serious threat to the environment and consequently affects plants, animals and human lives (Gupta and Saleh, 2013). Water contamination and poor sanitation are linked to the transmission of diseases such as cholera, typhoid, dysentery and hepatitis A (Ashbolt, 2004). Water pollutants are mainly organic and inorganic pollutants that are discharged from industrial effluents and sewage into the water bodies (Wasewar *et al*., 2020). Organic pollutants are primarily of carbon and hydrogen compounds which include dye, phenolic compounds, petroleum, surfactants, pesticides, and pharmaceuticals (Chowdhury *et al*., 2016). Dye is one of the major contaminants of great concern because of its complex structures which make them more resistant to biodegradation (Abdullah *et al*., 2018; Iqbal *et al*., 2021). Synthetic dyes are increasingly used in manufacturing operations such as leather, textiles, cosmetics, paper, printing, electroplating, plastics, and pharmaceuticals as industrial civilization progresses (Zhang *et al.,* 2018). They find their way into water bodies as a result of indiscriminate discharge of the effluents of the aforementioned industries. Water contamination by dye-laden effluent is easily observed due to its colour even at very little concentration. Dyes can also irritate the skin and induce allergic dermatitis. Several of them are carcinogenic and mutagenic to aquatic creatures (Meroufel *et al*., 2013). Congo red (CR) dye is a water-soluble anionic dye that is commonly used in the textile, paper, printing, leather, and plastic industries. Its principal negative effects are irritation of the eyes and skin (Malik *et al*., 2020).

Corresponding Author Email: bello.mo@unilorin.edu.ng

Long-term negative effects of ingestion of congo red dye are the destruction of the blood system, liver, and hematopoiesis, causing health problems such as breathing difficulties, diarrhoea, vomiting, and nausea (Munagapati and Kim, 2017). Among the conventional treatment methods of industrial effluent which include flocculation, coagulation and adsorption (Kannan and Meenakshisundaram, 2002), adsorption is often regarded as one of the most appealing techniques due to its great efficiency, ease of operation, and low cost, (Chikri *et al*., 2020; Dutta *et al*., 2021). The most commonly used adsorbent for the treatment of effluents is activated carbon. However, there is a high cost of production associated with the use of activated carbon (Ali *et al*., 2012). This has led to the investigation of different materials by researchers to be used as low-cost and effective adsorbents. Metallic oxides such as iron oxide, zinc oxide alumina, silica, clay and zeolite have been reported as adsorbents for the removal of pollutants from water. Zinc oxide (ZnO) is a low-cost material and that can be produced on a large scale (Zhang *et al.,* 2013). ZnO has received significant attention owing to its exclusive electrical, optical, and chemical properties (Nassef *et al.,* 2020). It has been applied to the removal of dyes like methylene blue (Nassef *et al.,* 2020), reactive blue and acid black (Khoshhesab and Souhani, 2018), congo red (Nayak *et al*., 2020) from aqueous solutions. Similarly, alumina is a common adsorbent that is environmentally stable (Asim *et al*., 2019). It exhibits a large surface area, high mechanical properties, and good resistance to heat (Reyes-lópez *et al*., 2021). Adsorption of some dyes such as methylene blue (Ali *et al.,* 2019), diresul black (Asim *et al*., 2019), orange G (Banerjee and Chattopadhyaya, 2017), orange 7 (Khosla *et al*., 2013) among others using alumina has been reported. This background information about the adverse effects of dye on environmental health together with the wide application of zinc oxide and alumina towards dye removal from aqueous solution instigated this present study. Herein, we report the adsorption study of a composite of zinc oxide and alumina (Al₂O₃/ZnO) as an adsorbent in comparison with zinc oxide alone.

MATERIALS AND METHODS

Materials: Aluminium cans were collected as municipal waste for the preparation of alumina. All chemicals used were of analytical grade. Zinc nitrate, sodium hydroxide, hydrochloric acid and congo red dye were purchased from BDH chemicals.

Preparation of ZnO: A modified method reported by Romadhan *et al*., (2016) and Suntako, (2015) was adopted. In a typical preparation, 250 ml of 0.5 M of zinc nitrate hexahydrate solution was measured and transferred into a beaker with a magnetic bar placed inside, 1 M of sodium hydroxide was added step-wisely until a pH of 13 was reached. This reaction was stirred constantly on a magnetic stirrer for 30 min at room temperature. The mixture was filtered, the residue was washed severally with aqueous ethanol and dried in an oven to obtain zinc oxide (ZnO) powder.

Preparation of Al₂O₃ from aluminium can: A slightly modified method reported by Chandra Shil, (2016) was employed. Herein, the colour inscription on the can was removed and then cut into smaller pieces. A 1 g of the pieces of aluminium was weighed and transferred into a beaker. This aluminium was leached with 100 ml of 6 M HCl in a conical flask on a magnetic stirrer in which Hydrogen gas (H₂) was evolved.

$$2Al + 6HCl \rightarrow 2AlCl_3 + 3H_{2(g)} \quad (1)$$

The obtained aluminium trichloride was filtered to remove the thin layer which was used to coat the aluminium, the filtrate was placed on a magnetic stirrer and 100 ml of 3 M NaOH was added step-wisely to form whitish precipitates of aluminium trihydroxides 2Al(OH)₃. The obtained precipitates were filtered and washed with deionized water. It was then dried and calcined at a temperature of 450 °C for 2 hr to yield aluminium oxide (Al₂O₃) in an electric furnace.

$$AlCl_3 + 3NaOH \rightarrow Al(OH)_3 + 3NaCl \quad (2)$$
$$Al(OH)_3 \underset{\Delta}{\rightarrow} Al_2O_3 \quad (3)$$
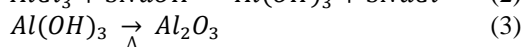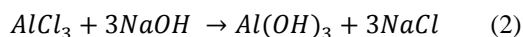
Preparation of Al₂O₃/ZnO composite: The composite was prepared by adopting a sol-gel method (Lakhera *et al*., 2015) using the earlier prepared Al₂O₃ and ZnO materials. A colloidal solution was formed by mixing 95 wt.% of ZnO and 5 wt.% of Al₂O₃ in deionized water. Each of the materials was dissolved separately in 50 ml of deionized water, stirred for 30 min and was added together with constant stirring on a magnetic stirrer at room temperature for 45 min. The mixture was filtered, washed and dried to obtain the Al₂O₃/ZnO composite.

Batch adsorption experiments: A batch adsorption method was employed (Abdus-Salam and Adekola, 2018). In acquiring typical adsorption data, 0.2 g of adsorbent was contacted with 20 ml of CR dye in a 50 ml conical flask reactor. The reactors were agitated on a mechanical shaker for a period of 2 hr at 25 °C. At equilibrium, the supernatant liquids were filtered and the filtrates were analyzed using UV

spectrophotometry (Jenway 7300/7305). The quantities adsorbed and percentages removed by the adsorbents were calculated using equations 4 - 6. The effects of concentration of CR (50 to 250 mg/L), contact time (5 to 120 min), adsorbent dosage (0.1 to 0.4 g) and temperature (25 to 45 °C) were investigated on the adsorption of congo red onto ZnO and Al₂O₃/ZnO composite.

$$q_e = \frac{C_o - C_e}{m} \; x \; V \qquad (4)$$

$$q_t = \frac{C_o - C_e}{m} \; x \; V \qquad (5)$$

$$\%_{rem} = \frac{C_o - C_e}{C_o} \; x100 \qquad (6)$$

Where q_e is the quantity adsorbed (mg/g), q_t is the quantity adsorbed at any time t (mg/g), c_o and c_e are the initial and equilibrium concentration respectively (mg/L), m is the mass of adsorbent (g) and V is the volume of adsorbate (L)

Isotherm study: The following isotherm models were used: Langmuir, Freundlich, Temkin and Dubinin-Radushkevich models.

Table 1: Isotherm equations

Isotherm model	Equation	Plot	Reference
Langmuir	$\frac{C_e}{q_e} = \frac{1}{q_m K_L} + \frac{C_e}{q_m}$ $R_L = \frac{1}{1+K_L C_o}$	$\frac{C_e}{q_e}$ vs C_e	(Abdus-Salam and Adekola, 2018)
Freundlich	$log q_e = log K_f + \frac{1}{n} \, log C_e$	$log q_e$ vs $log C_e$	(Bello *et al.*, 2021)
Temkin	$q_e = \beta ln k_T + \beta ln C_e$ $\beta = \frac{RT}{b}$	q_e vs $ln C_e$	(Inyinbor *et al.*, 2016)
Dubinin-Radushkevich	$ln q_e = ln q_s - K_D \varepsilon^2$ $\varepsilon = RT ln(1 + \frac{1}{C_e})$ $E = \frac{1}{\sqrt{2K_{ad}}}$	$ln q_e$ vs ε^2	(Inyinbor *et al.*, 2016)

Where q_e (mg/g) is the amount of CR dye adsorbed; C_e (mg/L) is the equilibrium concentration of the dye; q_m (mg/g) is the monolayer adsorption capacity; K_L (L/mg) is the Langmuir constant; K_f (mg/g) is the Freundlich constant; n is the empirical parameter which is related to the sorption intensity; K_t (L/mg) is the equilibrium binding constant corresponding to the maximum binding energy; β (J/mol) is related to the heat of adsorption; R is gas constant (8.314 J/mol.K); T (K) is the absolute temperature; q_s (mg/g) is the theoretical adsorption capacity; K_{ad} (mol²/kJ²) is the Dubinin–Radushkevich isotherm constant; $\mathcal{E}$ is the adsorption potential and E (kJ/mol) is the mean adsorption energy.

Table 2: Kinetic equations

Kinetic model	Equation	Plot	Reference
Pseudo-first-order	$log(q_e - q_t) = log q_e - \frac{k_1 t}{2.303}$	$log(q_e - q_t)$ vs t	(Pathania *et al.*, 2017)
Pseudo-second-order	$\frac{t}{q_t} = \frac{1}{K_2 q_{e^2}} + \frac{1}{q_e} t$	$\frac{t}{qt}$ vs t	
Intra-particle diffusion	$q_t = k_i t^{0.5} + c$	q_t vs $t^{0.5}$	(Liu *et al.*, 2019)
Elovich	$q_t = \frac{1}{\beta} \ln(\alpha\beta) + \frac{1}{\beta} \, lnt$	q_t vs lnt	(Ahmad *et al.*, 2019)

Where q_e and q_t (mg/g) are the amounts of CR dye adsorbed at equilibrium and at time t (min), respectively; k_1 (min⁻¹) is the adsorption rate constant for pseudo-first-order; k_2 (g m/g min) is the rate constant of pseudo-second-order adsorption; k_i (mg/g.min^{0.5}) is the intra-particle diffusion rate constant; C is the intercept related to the thickness of the boundary layer; α (mg/g.min) is the initial sorption rate and β (g/mg) is related to the extent of surface coverage and activation energy for chemisorption.

Table 3: Van't Hoff equation

Model	Equation	Plot	Reference
Van't Hoff	$ln k_c = -\frac{\Delta H^0}{RT} + \frac{\Delta S^0}{R}$ $k_c = \frac{C_{ads}}{C_e}$ $\Delta G^0 = \Delta H^0 - T\Delta S^0$	$ln k_c$ vs $\frac{1}{T}$	(Abdus-Salam and Adekola, 2018)

Where k_c is the equilibrium constant, C_e (mg/L) is the equilibrium concentration of adsorbate in solution, and C_{ads} (mg/L) is the concentration on adsorbent at equilibrium. ΔG^o, ΔH^o and ΔS^o are changed in Gibbs free energy (kJ/mol), enthalpy (kJ/mol) and entropy (J/mol.K) respectively; R is the gas constant (8.314 J/mol.K) and T (K) is the temperature.

Kinetic study: Four kinetic models were employed for the treatment of the data, which are pseudo-first-order (PFO), pseudo-second-order (PSO), intra-particle diffusion (IPD) and Elovich models.

Thermodynamic study: The variation in the adsorption equilibrium constant with temperature is usually studied by applying Van't Hoff equation, which is presented in table 3.

BELLO, MO; OYEWUMI-MUSA, RT; ABDUS-SALAM, N; GBENRO MT; EGBENEYE OG

RESULTS AND DISCUSSION

Characterisation: Surface functional group: The FTIR spectra of ZnO and Al_2O_3 are presented in Fig. 1. The surface of the prepared individual ZnO and Al_2O_3 is characterised by similar functional groups with a slight shift. For ZnO (a), the metal-oxygen bond which suggests Zn-O is observed at 894 and 461 cm^{-1}. The broad band at 3464 cm^{-1} is due to O-H stretching of the absorbed water molecule (Sowri Babu *et al*., 2013). The peak observed for Al_2O_3 (b) at 3450 cm^{-1} is due to O-H stretching of the absorbed water molecule. Al-O bonds of boehmite are attributed to peaks at 992, 552 and 455 cm^{-1} (Liu *et al*., 2012). The peak at 1634 and 1642 cm^{-1} for ZnO and Al_2O_3 respectively indicate -OH bending (Gupta *et al*., 2011). Similarly, the peaks at 1384 and 1453 cm^{-1} for ZnO and Al_2O_3 respectively are likely due to CO_2 absorption.
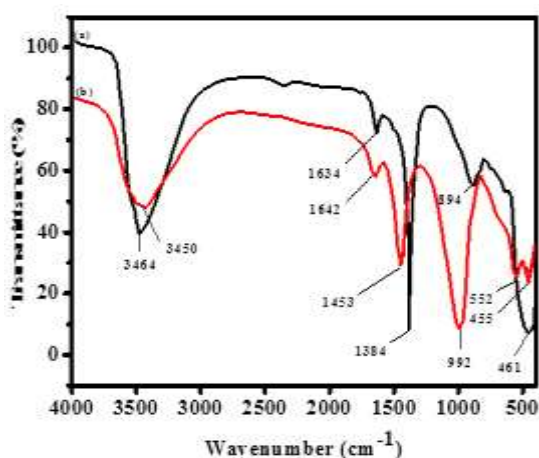

Fig. 1: FTIR spectra of (a) ZnO and (b) Al_2O_3

Surface morphology and elemental composition: The surface morphologies of ZnO, Al_2O_3 and Al_2O_3/ZnO are presented in Fig. 2. Roughly small particles characterised the surface of ZnO while that of Al_2O_3 showed bigger flake-like particles. The composite, however, showed agglomeration of particles resulting in a big rigid particle on its surface. The elemental compositions as revealed by energy dispersive x-ray (EDX) showed the expected elemental compositions in ZnO and Al_2O_3. The presence of Al and Zn are also observed in the composite (Al_2O_3/ZnO).

Adsorption studies: *Effect of concentration and isotherm study*: The adsorption capacities of ZnO and Al_2O_3/ZnO increased with an increase in the concentration of CR dye as presented in Fig. 3. The increase in quantity adsorbed by the two adsorbents is due to the increase in the gradient between the adsorbents and the dye molecules as the concentration increases (Akkaya Sayіili, 2015). Both adsorbents competed favourably for the removal of CR dye molecules from aqueous solutions at a lower concentration between 50 mg/L and 150 mg/L. However, Al_2O_3/ZnO composite material showed little improvement over ZnO between 200 mg/L and 250 mg/L of CR dye. The maximum adsorption capacities at 250 mg/L are 24.33 mg/g (97.28%) and 24.57 mg/g (97.35%) for ZnO and Al_2O_3/ZnO respectively. The adsorption of congo red (CR) dye onto ZnO and Al_2O_3/ZnO can be best described by Langmuir isotherm with the coefficient of correlation (R^2) of 0.9972 and 0.9681 respectively (Table 4). The order of fitness of the adsorption data to the isotherm model is Freundlich < Dubinin-Radushkevich < Temkin < Langmuir for the two adsorbents. The fitness of the adsorption data to the Langmuir model suggests monolayer adsorption (Banerjee and Chattopadhyaya, 2017). The estimated monolayer maximum adsorption capacity (q_m) showed that Al_2O_3/ZnO performed better than ZnO. The adsorption of CR dye onto the adsorbents is favourable as revealed by the value of the dimensionless factor, R_L. Value of R_L between 0 and 1 is an appropriate condition (Batool *et al*., 2018). The heat of adsorption from the Temkin model, 5.860 and 7.594 J/mol for ZnO and Al_2O_3/ZnO respectively suggest that the adsorption of CR dye is physisorption. The position is also supported by the value of adsorption energy (E) obtained for ZnO (2.461 kJ/mol) and Al_2O_3/ZnO (2.104 kJ/mol) from the Dubinin-Radushkevich model. The extent of energy between 0 and 8 kJ/mol is said to be physisorption while the adsorption is chemisorption when it ranges between 8 and 16 kJ/mol (Das *et al*., 2014). Comparing the values of q_s (mg/g) which is related to the theoretical adsorption capacity, it is also observed that Al_2O_3/ZnO performed better than ZnO. The Freundlich model suggests that a heterogeneous surface of the adsorbents cannot be ruled out of the process as it also gave significant R^2 values.

Effect of contact time and kinetics study: The effect of contact time between the adsorbate (100 mg/L of CR dye) and the adsorbents (ZnO and Al_2O_3/ZnO) is presented in Fig. 4. The adsorption of CR dye onto ZnO and Al_2O_3/ZnO was rapid at the initial stage of the process (0 – 15 min). Thereafter, the rate of adsorption slowed down towards equilibrium at 45 min. The adsorption sites of the adsorbents were readily available at the initial stage thereby making the removal process faster and slowed down when the adsorption sites have been saturated (Banerjee and Chattopadhyaya, 2017; Kurniawati *et al*., 2021). At 15 min, 8.53 mg/g (85.32%) and 9.26 mg/g (92.57%) of CR molecules were adsorbed onto ZnO and Al_2O_3/ZnO respectively.
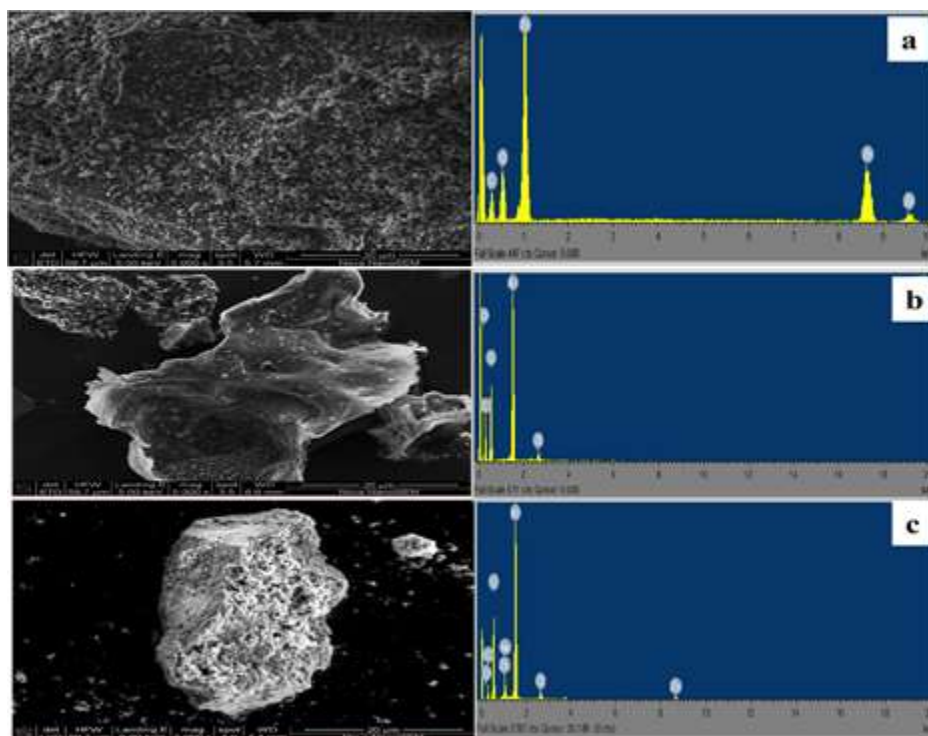
Fig. 2. SEM-EDX spectra of (a) ZnO (b) Al$_2$O$_3$ and (c) Al$_2$O$_3$/ZnO

The kinetics study using four models (Table 5) shows that pseudo-second-order (PSO) with the highest R^2 values for both adsorbents best described the adsorption kinetics, suggesting physicochemical interaction between adsorbate and adsorbent. Also, the calculated quantities adsorbed (q$_{e, cal}$) are in closed value with the one obtained experimentally (q$_{e, exp}$). The rate constant k$_2$ indicates that the adsorption process is faster onto Al$_2$O$_3$/ZnO (0.093 min^{-1}) than ZnO (0.049 min^{-1}). The higher the rate constant k$_2$, the faster is the reaction (Liu *et al.,* 2019). The good fitting showed by the pseudo-first-order (PFO) model is suggesting that the physical interaction of the adsorbate and adsorbent cannot be overlooked (Bello *et al.*, 2021). The intra-particle diffusion (IPD) model plot did not pass through the origin (Fig. not shown) but the confirmation of its existence is the significant R^2 values for ZnO (0.7235) and Al$_2$O$_3$/ZnO (0.7449). Consequently, intra-particle diffusion is not the only rate-controlling step for the adsorption of CR dye onto the adsorbents (Yakout and Elsherif, 2010). Elovich model which is used to describe chemisorption (Wu *et al.*, 2009) showed the least but moderate R^2 values suggest that chemical interaction cannot be excluded in the process.

Effect of adsorbent dosage: The determination of the best performing adsorbent dosage is important to reduce the wastage of adsorbent and for optimum process efficiency (Iqbal *et al*., 2021). Fig. 5 shows the

effect of adsorbent dosage on the adsorption of CR dye (100 mg/L) onto ZnO and Al$_2$O$_3$/ZnO composite.
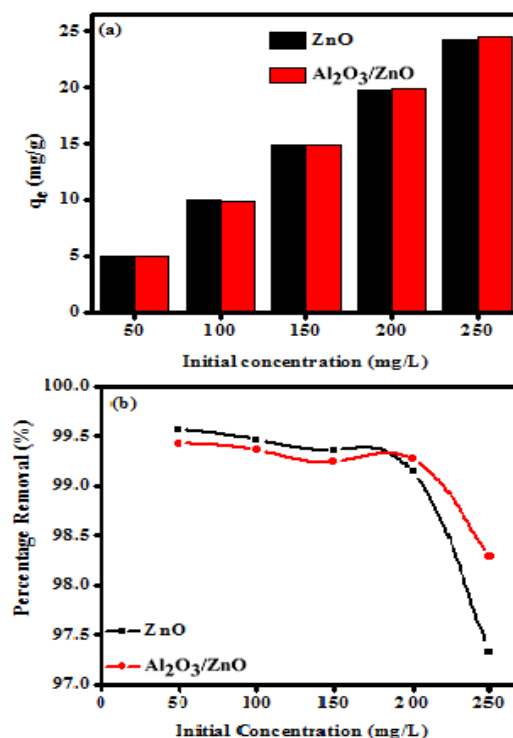

It was observed that the quantity of CR dye adsorbed decreased with an increase in the adsorbents (ZnO and Al$_2$O$_3$/ZnO) dosage. The overlapping and unsaturation

of the adsorption sites as the quantity of the adsorbent was increased while the concentration of dye molecule remained constant were the likely causes of the reduction (Etim *et al*., 2016; Zhu *et al*., 2017).

**Table 4:** Isotherm parameters for adsorption of CR dye onto ZnO and Al₂O₃/ZnO

Model/Parameters		Value	
		ZnO	Al₂O₃/ZnO
Langmuir	q_m (mg/g)	27.67	33.39
	K_L (L/g)	1.151	0.703
	R_L	0.0034	0.0057
	R^2	0.9972	0.9681
Freundlich	K_f (mg/g)	0.041	0.040
	n	2.172	1.658
	R^2	0.8537	0.8893
Temkin	K_r (L/mg)	11.91	6.682
	β (J/mol)	5.860	7.594
	B	422.75	326.25
	R^2	0.9559	0.9512
Dubinin-Radushkevich	q_s (mg/g)	21.08	22.02
	K_{ad} (mol²/kJ²)	8.25×10^{-8}	1.13×10^{-7}
	E (kJ/mol)	2.461	2.104
	R^2	0.9358	0.9321
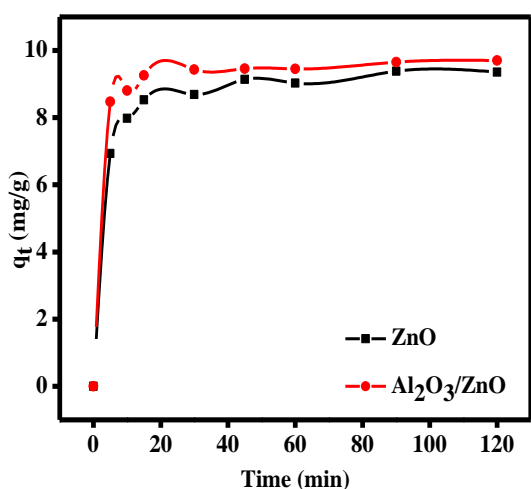
Fig. 4: Effect of contact time on quantity of CR dye adsorbed

Table 5: Kinetic parameters for adsorption of CR dye onto ZnO and Al₂O₃/ZnO

Model/Parameters		Value	
		ZnO	Al₂O₃/ZnO
PFO	$q_{e, exp}$ (mg g⁻¹)	9.38	9.70
	$q_{e, cal}$ (mg g⁻¹)	0.49	0.99
	k_1 (min⁻¹)	0.0055	0.0061
	R^2	0.7645	0.8221
PSO	$q_{e, exp}$ (mg g⁻¹)	9.38	9.70
	$q_{e, cal}$ (mg g⁻¹)	9.54	9.75
	k_2 (g mg⁻¹ min⁻¹)	0.049	0.093
	R^2	0.9997	0.9999
IPD	C	7.1749	8.5188
	k_i (mg g⁻¹ min⁻⁰·⁵)	0.235	0.1224
	R^2	0.7235	0.7449
Elovich	α (g mg⁻¹ min⁻¹)	1.16×10^{11}	3.05×10^9
	β (mg g⁻¹)	1.41	2.72
	R^2	0.6896	0.6427
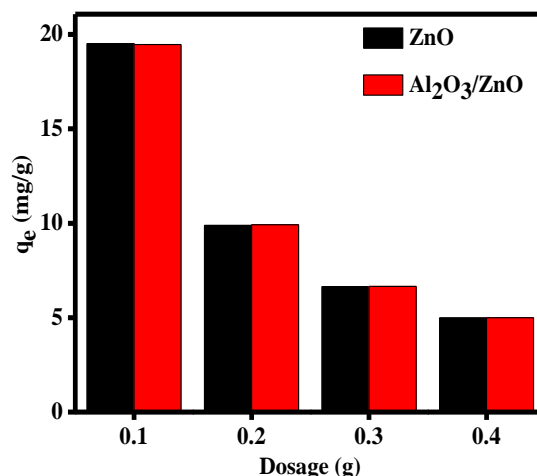
Fig. 5: Effect of adsorbent dosage on quantity of CR dye adsorbed

Effect of temperature and thermodynamic study: The effect of temperature on the adsorption of CR dye (100 mg/L) onto ZnO and Al₂O₃/ZnO composite is presented in Fig. 6. It was observed that the quantity adsorbed increased with an increase in temperature from 25 to 45 ℃, indicating an endothermic process. The endothermic nature of the adsorption process is attributed to an increase in the kinetic energy of the dye molecules and they moved faster towards the adsorption sites (Jiang *et al*., 2018). A similar observation for adsorption of CR dye onto adsorbent derived from shrimp shells was reported by Zhou *et al*., (2018).
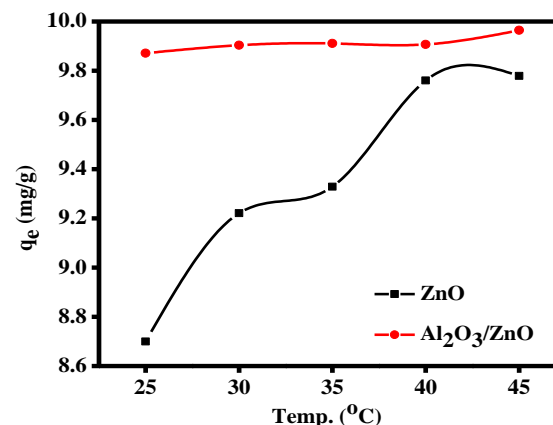
Fig. 6: Effect of temperature on quantity of CR dye adsorbed

The thermodynamic parameters obtained from van't Hoff plot are presented in Table 6. The thermodynamic study of the adsorption process agrees with the endothermic nature observed in the experiment with positive enthalpy change (ΔH) of 78.9 kJ/mol and 40.94 78.9 kJ/mol for ZnO and Al₂O₃/ZnO respectively. The lower ΔH for adsorption of CR onto the composite is an indication of its enhanced performance over ZnO. This is supported by

the spontaneity of the reaction as suggested by more negative values of ΔG for Al_2O_3/ZnO than ZnO. However, both are spontaneous within the range of temperature studied. The positive degree of disorderliness (ΔS) for both adsorbent indicates that the adsorption is controlled by the entropy effect (Zhou *et al.*, 2018).

Table 6: Thermodynamic parameters for adsorption of CR dye onto ZnO and Al_2O_3/ZnO

Adsorbent	ΔH (kJ/mol)	ΔS (kJ/molK)	ΔG (kJ/mol)				
			298K	303K	308K	313K	318K
ZnO	78.94	0.280	-4.659	-6.062	-7.466	-8.868	-10.271
Al_2O_3/ZnO	40.94	0.172	-10.576	-11.440	-12.305	-13.169	-14.034

Conclusion: The removal of congo red dye from aqueous solution using the prepared ZnO and Al_2O_3/ZnO composite was achieved by adsorption process. The isotherm parameters suggested physisorption and monolayer interaction between the adsorbate and the adsorbents. Kinetic and thermodynamic data indicated physicochemical, surface interaction, intra-particle diffusion and spontaneous adsorption process. The Al_2O_3/ZnO composite showed a slight improvement over ZnO alone, indicating the impact of the Al_2O_3.

REFERENCES

Abdullah, N; Tajuddin, MH., Yusof, N (2018). Carbon-based polymer nanocomposites for dye and pigment removal. *Carbon-Based Polym. Nanocomposites Environ. Energy Appl*. 305-329.

Abdus-Salam, N; Adekola, SK (2018). Adsorption studies of zinc (II) on magnetite, baobab (Adansonia digitata) and magnetite–baobab composite. *Appl. Water Sci.*, 8(8): 222–232.

Ahmad, MA; Ahmed, NB; Adegoke, KA; Bello, OS (2019). Sorption studies of methyl red dye removal using lemon grass (Cymbopogon citratus). *Chem. Data Collect.*, *22*, 100249.

Akkaya Saylili, G (2015). Synthesis, characterization and adsorption properties of a novel biomagnetic composite for the removal of Congo red from aqueous medium. *J. Mol. Liq*. 211: 515-526.

Ali, I; Asim, M; Khan, TA (2012). Low cost adsorbents for the removal of organic pollutants from wastewater. *J. Envirn Manage*. 113: 170-183.

Ali, S; Abbas, Y; Zuhra, Z; Butler, IS (2019). Synthesis of γ-alumina (Al_2O_3) nanoparticles and their potential for use as an adsorbent in the removal of methylene blue dye from industrial wastewater. *Nanoscale Adv*. 1: 213-218.

Ashbolt, NJ (2004). Microbial contamination of drinking water and disease outcomes in developing regions. *Toxicology*. 198(1-3): 229-238.

Asim, T; Mamoona, M; Tahir, A; Nisar, N; Ali, A; Sheikh, A (2019). Alumina as environmentally stable adsorbent for the removal of diresul black dye from waste water. *Water Pract. and Technol*. 14(1) 62-70.

Banerjee, S; Chattopadhyaya, MC (2017). Adsorption characteristics for the removal of a toxic dye, tartrazine from aqueous solutions by a low cost agricultural by-product. *Arab. J. Chem*. 10: S1629-S1638.

Batool, F; Akbar, J; Iqbal, S; Noreen, S; Bukhari, SNA (2018). Study of Isothermal, Kinetic, and Thermodynamic Parameters for Adsorption of Cadmium: An Overview of Linear and Nonlinear Approach and Error Analysis. *Bioinorg. Chem. Appl*. https://doi.org/10.1155/2018/3463724

Bello, MO; Abdus-Salam, N; Adekola, FA; Pal, U (2021). Isotherm and kinetic studies of adsorption of methylene blue using activated carbon from ackee apple pods. *Chem. Data Collect*. 31, 100607.

Chandra Shil, T (2016). Preparation of Aluminum Oxide from Industrial Waste Can Available in Bangladesh Environment: SEM and EDX Analysis. *J. Adv. Chem. Eng*. 6(152):1-5.

Chikri, R; Elhadiri, N; Benchanaa, M; El maguana, Y (2020). Efficiency of sawdust as low-cost adsorbent for dyes removal. *J. Chem*. https://doi.org/10.1155/2020/8813420

Chowdhury, S; Khan, N; Kim, G. H; Harris, J; Longhurst, P; Bolan, NS (2016). Zeolite for Nutrient Stripping From Farm Effluents. *Environ.*

Mat. Waste: Res. Recover. Pollut. Prev. 569-589.

Das, B; Mondal, NK; Bhaumik, R; Roy, P (2014). Insight into adsorption equilibrium, kinetics and thermodynamics of lead onto alluvial soil. *Int. J. Environ. Sci. Technol*, 11(4): 1101–1114.

Dutta, S; Gupta, B; Srivastava, SK;Gupta, AK (2021). Recent advances on the removal of dyes from wastewater using various adsorbents: A critical review. *Mat. Adv*. 2: 4497-4531.

Etim, UJ; Umoren, SA; Eduok, UM (2016). Coconut coir dust as a low cost adsorbent for the removal of cationic dye from aqueous solution. *J. Saudi Chem.Soc*. 20: S67–S76.

Gupta, S; Ramamurthy, PC; Madras, G (2011). Synthesis and characterization of flexible epoxy nanocomposites reinforced with amine functionalized alumina nanoparticles: A potential encapsulant for organic devices. *Polym. Chem.* 2(1): 221-228.

Gupta, VK; Saleh, TA (2013). Sorption of pollutants by porous carbon, carbon nanotubes and fullerene- An overview. *Environ. Sci. Pollut. Res*. 20(5): 2828-2843.

Inyinbor, AA; Adekola, FA; Olatunji, GA (2016). Kinetics, isotherms and thermodynamic modeling of liquid phase adsorption of Rhodamine B dye onto Raphia hookerie fruit epicarp. *Water Resour. Ind.*. 15: 14–27.

Iqbal, MM; Imran, M; Hussain, T; Naeem, MA; Al-Kahtani, AA; Shah, GM; Ahmad, S; Farooq, A; Rizwan, M; Majeed, A; Khan, AR; Ali, S (2021). Effective sequestration of Congo red dye with ZnO/cotton stalks biochar nanocomposite: Modeling, reusability and stability. *J. Saudi Chem. Soc.* 25(2): 2020.101176

Jiang, LL; Yu, HT; Pei, LF; Hou, XG (2018). The effect of temperatures on the synergistic effect between a magnetic field and functionalized graphene oxide-carbon nanotube composite for Pb^{2+} and phenol adsorption. *J. Nanomater.*1-13.

Kannan, N; Meenakshisundaram, M (2002). Adsorption Of Congo Red On Various Activated Carbons. A Comparative Study. *Water Air and Soil Pollut*. 138: 289-305.

Khosla, E; Kaur, S; Dave, PN (2013). Mechanistic study of adsorption of acid orange-7 over aluminum oxide nanoparticles. *J. Eng.* https://doi.org/10.1155/2013/593534

Kurniawati, D; Bahrizal, Sari, TK; Adella, F; Sy, S (2021). Effect of Contact Time Adsorption of Rhodamine B, Methyl Orange and Methylene Blue Colours on Langsat Shell with Batch Methods. *J. Phys: Conf. Ser*. 1788.

Lakhera, SK; Harsha, S; Suman, AS (2015). Synthesis and characterization of 13X zeolite/activated carbon composite. *Int. J. ChemTech Res*. 7: 1364–1368.

Lellis, B; Fávaro-Polonio, CZ; Pamphile, JA; Polonio, JC (2019). Effects of textile dyes on health and the environment and bioremediation potential of living organisms. *Biotechnol. Res. and Innov*. 3(2): 275-290.

Liu, C; Shih, K; Gao, Y; Li, F; Wei, L (2012). Dechlorinating transformation of propachlor through nucleophilic substitution by dithionite on the surface of alumina. *J. Soils Sediments*.12: 724-733.

Liu, QX.; Zhou, YR.; Wang, M; Zhang, Q; Ji, T; Chen, TY; Yu, DC (2019). Adsorption of methylene blue from aqueous solution onto viscose-based activated carbon fiber felts: Kinetics and equilibrium studies. *Adsorpt. Sci. Technol*. 37(3–4): 312–332.

Malik, A; Khan, A; Anwar, N; Naeem, M (2020). A comparative study of the adsorption of congo red dye on rice husk, rice husk char and chemically modified rice husk char from aqueous media. *Bull. Chem. Soc. of Ethiop*. 34(1): 41-54.

Meroufel, B; Benali, O; Benyahia, M; Benmoussa, Y; Zenasni, MA (2013). Adsorptive removal of anionic dye from aqueous solutions by Algerian kaolin : Characteristics , isotherm , kinetic and thermodynamic studies. *J. Mat. Environ. Sci.* 4(3): 482–491.

Monsef Khoshhesab, Z; Souhani, S (2018). Adsorptive removal of reactive dyes from aqueous solutions using zinc oxide nanoparticles. *J. Chinese Chem. Soc*. 65(12): 1482-1490.

Munagapati, VS; Kim, DS (2017). Equilibrium isotherms, kinetics, and thermodynamics studies for congo red adsorption using calcium alginate beads impregnated with nano-goethite. *Ecotoxicol. Environ. Saf*. 141:226-234.

Nassef E; Yousef NS; Farouq R (2020). Adsorption of Dye by Nano-zinc oxide. *J. Am. Sci*. 3(16), 81–89.

Nayak, A; Sahoo, JK.; Sahoo, SK (2020). Removal of congo red dye from aqueous solution using zinc oxide nanoparticles synthesised from Ocimum sanctum (Tulsi leaf): a green approach. *Int. J. Environ. Anal. Chem.* 1–22.

Pathania, D; Sharma, S; Singh, P (2017). Removal of methylene blue by adsorption onto activated carbon developed from Ficus carica bast. *Arab J. Chem.* 10: S1445–S1451.

Reyes-lópez, SY; Aguirre-terrazas, KA; Torres-pérez, J; Nahúm, M; Ruíz-baltazar, ÁDJ (2021). Review of Alumina in Adsorption Processes for Emerging Pollutants. *Int. J. Res.* 9(4): 435-453.

Romadhan, M; Suyatma, NE; Taqi, FM (2016). Synthesis of ZnO nanoparticles by precipitation method with their antibacterial effect. *Indones. J. Chem*. 16(2): 117-123.

Sowri Babu, K.; Ramachandra Reddy, A; Sujatha, C; Venugopal Reddy, K; Mallika, AN (2013). Synthesis and optical characterization of porous ZnO. *J. Adv. Ceram*. 2: 260-265.

Suntako, R (2015). Effect of zinc oxide nanoparticles synthesized by a precipitation method on mechanical and morphological properties of the CR foam. *Bull. Mat. Sci*. 38: 1033-1038.

Wasewar, KL; Singh, S; Kansal, SK (2020). Process intensification of treatment of inorganic water pollutants. *Inorg. Pollut. Water*. 245-271.

Wu, FC; Tseng, RL; Juang, RS (2009). Characteristics of Elovich equation used for the analysis of adsorption kinetics in dye-chitosan systems. *Chem. Eng. J.* 150 (2–3): 366–373.

Yakout, SM; Elsherif E (2010). Batch kinetics, isotherm and thermodynamic studies of adsorption of strontium from aqueous solutions onto low cost rice-straw based carbons. *Carbon - Sci. Technol*.3, 144-153.

Zhang, F; Lan, J; Yang, Y; Wei, T; Tan, R; Song, W (2013). Adsorption behavior and mechanism of methyl blue on zinc oxide nanoparticles. *J. Nanoparticle Res*. 15(11): 2034-2

Zhang, Z; Li, Y; Du, Q; Li, Q (2018). Adsorption of Congo Red from Aqueous Solutions by Porous Soybean Curd Xerogels. *Polish J. Chem. Technol*. 20(3): 95-102.

Zhou, Y; Ge, L; Fan, N; Xia, M (2018). Adsorption of Congo red from aqueous solution onto shrimp shell powder. *Adsorpt. Sci. Technol*. 36(5-6): 1310-1330.

Zhu, M; Tian, W; Chai, H; Yao, J (2017). Acid-hydrolyzed agricultural residue: A potential adsorbent for the decontamination of naphthalene from water bodies. *Korean J. Chem. Eng*. 34(4): 1073–1080.